

UCLA

UCLA Electronic Theses and Dissertations

Title

Role of Beclin1 in osteocytes and lacunar-canalicular network

Permalink

<https://escholarship.org/uc/item/0b85j3v4>

Author

Jung, Da Hae

Publication Date

2022

Peer reviewed|Thesis/dissertation

UNIVERSITY OF CALIFORNIA

Los Angeles

Role of Beclin1 in osteocytes and lacunar-canalicular network

A thesis submitted in partial satisfaction

of the requirements for the degree Master of Science

in Oral Biology

by

Da Hae Jung

2022

© Copyright by

Da Hae Jung

2022

ABSTRACT OF THE THESIS

Role of Beclin1 in osteocytes and lacunar-canalicular network

by

Da Hae Jung

Master of Science in Oral Biology

University of California, Los Angeles, 2022

Professor Reuben Han-Kyu Kim, Chair

Autophagy is identified as a key player in physiological processes and progression of many pathological conditions such as metabolic dysregulation, neurodegenerative disorders, aging, cancer, and bone related diseases. Recent studies showed that autophagy plays important roles in bone homeostasis by regulating bone-related cells such as osteoblasts and osteoclasts. However, less is known about the role of autophagy in osteocytes. As our ongoing effort to examine the role of autophagy in osteocytes, our laboratory previously generated osteocyte-specific conditional

Beclin1 knockout mice. Here, we examined the role of Beclin1, one of the master regulators of the autophagic pathway, in the lacunar-canalicular network (LCN) and pericanalicular remodeling (PLR) *in vivo* and *in vitro*. Silver nitrate staining of the femurs showed

significant decreases in canalicular length and density. Becn1 was knocked down (KD) in immortalized osteocytes, MLO-Y4 cells using lentiviral infection. Becn1 KD MLO-Y4 cells exhibited more rounded phenotypes and suppressed autophagy-related genes (Atgs) as well as protein expression of LC3B, a marker for autophagy. Becn1 KD MLO-Y4 cells also showed reduced gene expression of PLR-associated genes such as Mmp2, Mmp9, Mmp13, Mmp14, and CtsK. CtsK expression was also reduced at the protein level. When cells were treated with TGF- β , a potent inducer of PLR-associated genes, the degree of induction was similar in Mmp2, Mmp9, Mmp13, and Serpine but reduced in Mmp14 and CtsK, suggesting that Becn1 may regulate PLR-associated gene expression in both TGF- β -dependent and -independent manner. Collectively, our study highlights the importance of Becn1 in osteocytes for regulating bone remodeling.

The thesis of Da Hae Jung is approved.

Bo Yu

Jimmy Kuanghsian Hu

Yousang Gwack

Reuben Han-Kyu Kim, Committee Chair

University of California, Los Angeles

2022

TABLE OF CONTENTS

1. INTRODUCTION	1
2. MATERIALS AND METHODS	4
3. RESULTS	8
4. DISCUSSION	12
5. FIGURE LEGENDS AND FIGURES	17
6. REFERENCE	29

Abbreviations

DMP1: Dentin matrix protein-1

Sost: Sclerostin

Fgf23: Fibroblast growth factor 23

RANKL: Receptor activator of nuclear factor kappa beta

OPG: Osteoprotegerin

Ctsk: Cathepsin K

TRAP: Tartrate resistant acid phosphatase

MEPE: Matrix extracellular phosphoglycoprotein

Mmp13: Matrix metalloproteinase 13

Phex: X-linked phosphate-regulating endopeptidase

Col1a1: Collagen type I alpha 1

Col3a1: Collagen type I alpha 1

LC3-I: Microtubule-associated protein light chain 3-I

LC3-II: Microtubule-associated protein light chain 3-II

1. Introduction

Autophagy is identified as a key player in physiological processes and progression of many pathological conditions such as metabolic dysregulation, neurodegenerative disorders, aging, cancer, and bone related diseases (Kimmelman *et al.*, 2017). Additionally, autophagy plays crucial role in bone homeostasis as it is responsible for regulating bone formation and recycling the process of cellular wastes. Autophagy is mainly subjected to capture and delivery of intracellular substances by forming autophagosomes which are composed by newly formed bilayer membranes, can surround unnecessary organelles and intracellular to process the cellular sequestration process. It is known that *Atgs* (autophagy-related genes) are heavily involved in the double-membrane vesicle formation as well as the delivery of cargos in autophagosomes to lysosomes (Levine *et al.*, 2019).

Among 20 identified *Atgs*-related proteins, *Atg6*, also known as *Beclin-1*, is an indispensable *Atg* that is responsible for initiation of autophagic process. *Beclin-1* plays a pivotal role for the phagophore formation and because it is a highly conserved mammalian protein, often utilized as a cellular autophagy marker (Fu *et al.*, 2013). Initially, *Beclin1* is identified as a tumor suppressor, it mediates a crosstalk between autophagic and apoptosis pathways by interrelating with antiapoptotic proteins including *Bcl-2*, *Bcl-X_L*, and *Mcl-1* through the BH3 domain (Maiuri,*et al.*, 2007). These antiapoptotic proteins get phosphorylated and detach from *Beclin1* upon activation of c-Jun N-terminal kinase (JNK) pathway and since RANKL activates JNK pathway, the activated JNK pathway potentially function in osteoclastogenesis by dissociating *Beclin1* from the antiapoptotic proteins and it becomes a “master” regulator for the sustained ATG activation during osteoclastogenesis (Liang *et al.*, 1999, Arai *et al.*, 2019).

Osteocytes are the most abundant (~95%) and longest living cells found in mature bone tissue to regulate osteoblast and osteoclast activities; however, it remains the least characterized cells in bone biology. Not only osteocytes are heavily responsible for regulating bone homeostasis, but osteocytes also form an abundance network of dendrites that communicate with approximately 50 neighboring osteocytes (Creecy *et al.*, 2021). MLO-4 cells are murine long bone osteocyte-like cells, these cells express RANKL ligand along their dendritic processes and secrete abundant amounts of macrophage colony-stimulating factor, both required for osteoclast formation (Bonewald *et al.*, 2008). Moreover, Bonewald *et al.*, suggest MLO-Y4 osteocytes do not undergo apoptosis are prevented from doing so by active protection mechanisms and lack sclerostin proteins, which is a negative regulator of bone formation, and can potently suppress inhibition of bone formation. Due to these characteristics, MLO-Y4 is an appropriate osteocyte-like cell line to investigate the role of *Becn1* in the molecular mechanism of autophagic pathway. Osteocyte cells are essentially embedded in the mineralized matrix in protected lacunae which surround the cell body. Those cells are linked to one another by dendritic cell processes in canaliculi and these form lacunar-canalicular network (LCN) in bone. Fluid flow through the perilacunar and canalicular spaces supports osteocyte cellular functions and secretion of osteoclast and osteoblast regulating molecules by which osteocytes impact bone remodeling, also activation or suppression of osteocyte mediated perilacunar/canalicular remodeling (PLR) (Asagiri *et al.*, 2007). Osteocytes resorb the mineral components of perilacunar and pericanalicular ECM through a combination of matrix metalloproteases (MMPs), ATPase proton pumps, and other enzymes including cathepsin K (CtsK) and carbonic anhydrases (Qing *et al.*, 2012).

Transforming growth factor-beta (TGF— β) pathway is a signaling pathways that regulates the bone mass and quality which released by bone-forming osteoblasts is sequestered in

the Extracellular Matrix of bone (ECM). The recent study demonstrated that not only TGF— β regulates the activity of osteoclasts and osteoblasts in bone homeostasis, but also osteocytes by regulating perilacunar/canalicular remodeling (PLR) in bone, during which they directly resorb and deposit bone matrix surrounding their lacuna-canalicular network (Qing *et al.*, 2009). Several studies have revealed that PLR affects changing in bone homeostasis and pathology. Fowler *et al.*, revealed that glucocorticoid specifically repress expression of PLR markers including *MMP2*, *MMP13*, *MMP14*, *CtsK*, *GILZ*, *L19* and more for osteocyte-mediated PLR. Moreover, a recent study also proved that the reduced estrogen levels increase bone turnover and induce bone loss due to larger effective lacunar-canalicular porosity around osteocytes in both cortical and cancellous bone (Sharma *et al.*, 2012). Nonetheless, the regulatory mechanisms of PLR by which osteocytes control bone remodeling, particularly in the context of autophagy, remain poorly understood.

As our ongoing effort to examine the role of Beclin1 in osteocytes, our lab previously generated osteocyte-specific conditional Beclin1 knockout mice by crossbreeding *Becn1^{f/f}* mice with *Dmp1^{+Cre}* mice (*Becn1^{f/f}; Dmp1^{+Cre}*, or simply Beclin1 cKO mice). These mice were born in Mendelian ratio without dramatic changes in bone phenotypes; however, *Becn1* cKO mice progressively gain bone thickness and density. Histologically, *Becn1* cKO mice exhibited reduced canalicular length and density in the Lacunar-canalicular network (LCN) of the cortical bone section in femur tissue. Here, we aimed to further examine the LCN phenotypes in *Becn1* cKO mice and to determine molecular mechanisms by which *Becn1* regulates expression of genes associated with osteocytes and LCN. To this end, we further evaluated LCN using silver nitrate staining, and we also conditionally knockdown *Becn1* in MLO-Y4 cells, osteocyte-like cells to examine the role of *Becn1* in autophagic pathway and PLR mechanism in bone homeostasis both *in vivo* and *in vitro*.

2. Materials and Methods

2.1 Mice

DMP1^{Cre/+} mice and Beclin^{f/f} mice were purchased from the Jackson Laboratories and Dr. Binfeng Lu (University of Pittsburgh School of Medicine) respectively. Then mice were born at the expected Mendalian ratio and generate Beclin^{f/f};DMP1^{Cre/+} mice. Beclin^{f/f};DMP^{+/+} (Beclin WT) mice and Beclin^{f/f};DMP1^{Cre/+} (Beclin cKO) mice were used for *in vivo* study. All mice were housed in the University of California, Los Angeles Division of Laboratory Animal Medicine. All experimental protocols were approved (ARC protocol #2012-033) by institutional guidelines from the UCLA Institutional Animal Care and Use Committee.

2.2 Tissue Harvest and Embedding

Femur tissues were harvested and fixed in 4% para-formaldehyde in PBS, pH 7.4 at 4°C overnight for tissue fixation. Upon completion of the μ CT scan, the femurs were decalcified in 5% EDTA/4% sucrose solution changed daily for two weeks. The tissues were then trimmed, and embedded in paraffin.

2.3 Micro-Computed tomography (CT) Scan

The fixed mice femurs were wrapped in 70% ethanol-soaked gauze, placed in a 15 mL centrifuge tube, and scanned in SkyScan 1275 (Bruker Micro-CT, Kontich, Belgium) at voxel size of 20 μm^3 and a 0.5 mm aluminum filter at 55 kVp and 145 μA , with an integration time of 200 ms

using a cylindrical tube (Field of view/Diameter: 20.48 mm). Femur tissues were reconstructed and analyzed using CTan and CTvol programs (Bruker μ CT, Kontich, Belgium) to generate 3D images and cross-sectional images.

2.4 Determination of lacunae and osteocyte lacuno-canalicular network

The embedded tissues were sectioned at mesiodistal plane at 5 micron thickness. With 20 sections from each tissue sample. All the slides used for the histomorphometric measurements were scanned at $\times 20$ and $\times 40$ using a high-resolution slide scanner (Aperio ScanScope AT, Buffalo Grove, IL) and were analyzed using an image analyzing software (Image J, NIH, USA) by a single investigator. The region of interest (ROI) was set as 3-mm cortical bone, beginning 1 mm apart from the growth plate. Lacunae were histologically categorized based on the presence or absence of nucleus of osteocytes on Hematoxylin and Eosin (H&E) stained cortical sections under $\times 20$ magnification. For determination of lacunae distribution, the cortical bone was divided into three areas as the outer cortex (O), middle cortex (M), inner cortex (I). Silver nitrate staining was done for visualization of the osteocyte lacuno-canalicular network in cortical bone. Canalicular length and density per lacuna of the middle cortex were evaluated under $\times 40$ magnification. The artifacts by sectioning or ossified lacunae were not counted.

2.5 Cells and Cell Culture

MLO-Y4 cells were purchased (EKC002, Kerfast, Inc.) and grew on culture plates coated with collagen (Rat tail collagen Type 1, 0.15mg/mL). Cells were seeded in cell plate

containing α -MEM (GIBCO, Carlsbad, CA, USA) supplemented with 2.5% Fetal Bovine Serum (Life Technologies), 2.5% Calf Serum (HyClone Laboratories), incubated at 38 Celsius, 5% CO₂ for 48 hours and the cells were harvested for RT-qPCR analysis.

2.6 shRNA Lentiviral Infection

The *Becn1* shRNAs lentiviral Particles (mouse, sc-29798-V) were purchased from Santa Cruz Biotechnology along with control shRNA lentiviral particles (sc-108080). Initially, MLO-Y4 cells were maintained in GIBCO's α -MEM supplemented with 2.5% fetal bovine serum, 2.5% calf serum, penicillin (100 U/mL) and streptomycin (100 μ g/mL). To infect MLO-Y4 cells, lentiviral particles were mixed with fresh serum medium and Polybrene (5 μ g/mL, Santa Cruz Biotechnology), applied to target cells and incubated for 6 hours. Cells were then fed with fresh, virus-free serum medium. 24 hours later, puromycin was added (2 μ g/mL). MLO-Y4 cells without any viral infection was used as a control, and puromycin was treated until all these cells are not viable.

2.7 RNA isolation and real-time quantitative RT-PCR (qRT-PCR)

Total RNA was isolated from the cultured cells using TRIzol® Reagent (ThermoFisher Scientific) and PureLink RNA Mini Kit (Invitrogen, Carlsbad, CA, USA) according to manufacturer's protocol. The quality of isolated mRNA was assessed using NanoDrop Spectrophotometer (ThermoFisher Scientific). Then, complementary DNA (cDNA) was synthesized from 2 μ g of total RNA extracted using SuperScript II FirstStrand Synthesis system

(Invitrogen) and Random Primer (Invitrogen). 2.0 μ L cDNA was amplified using SYBR Green I Master Mix (Roche Applied Sciences) with the LightCycler 480 real-time PCR system with primers for Atg6 Becn-1 and GAPDH was used as internal control. The cDNA was loaded in triplicates in LightCycler 96 well plates (Roche Applied Sciences). Second derivatives Cq values of the genes and GAPDH were compared to assess the fold differences of amplification following the manufacturer's instruction (Roche Applied Sciences).

2.8 Western Blotting

The medium was removed, and cells were harvested in 6 well cell plate. Cells were lysed using 0.1% NP-40 lysis buffer [20 mM Tris (pH 7.5), 50 mM Beta-glycerophosphate, 150 mM NaCl, 1 mM EDTA, 25 mM NaF, 1 mM Na₃VO₄, 16 protease inhibitor cocktail (Sigma-Aldrich), 16 phosphatase inhibitor cocktail I (Sigma-Aldrich), and 16 phosphatase inhibitors cocktail I (Sigma-Aldrich), phosphatase inhibitor cocktail II (Sigma-Aldrich)]. Lysates (40 to 50 mg) from cells were used for immunoprecipitation and Western blot analysis and fractionated by 12% sodium dodecyl sulfate-polyacrylamide gel electrophoresis and transferred onto the Immobilon protein membrane (Millipore, Billerica, MA, USA). The immobilized membrane was incubated with anti-ALP antibody (H-300; Santa Cruz Biotechnology) and probed with the respective secondary antibody. The membrane was exposed to the HyGLO chemiluminescent HRP antibody detection reagent (Denville Scientific, South Plainfield, NJ, USA) and scanned using the ChemiDoc system (Bio-Rad Laboratories, Hercules, CA, USA).

2.9 Statistical analysis

Results were expressed as Mean \pm standard deviation in bar diagrams. The significance of difference between means with single variable was analyzed by student t-test. The value of $p < 0.05$ was considered to be statistically significant in all statistical analyses. All the statistical tests were performed with Graph Pad Prism 6 software (La Jolla, CA, USA).

3. Results

3.1 *Becn-1* regulates lacunae and canaliculi network (perilacunar/canalicular remodeling)

Silver-nitrate-stained assay was utilized on femoral cortical bone of 6 months-old Wildtype (n=6) and *Becn1* conditional KO mice (n=5) to evaluate the osteocyte lacuna-canalicular network and the canalicular length. Distinctly, the osteocyte canalicular network of *Becn1* cKO mice has markedly decreased as compared to the control mice (**Figure 1**). Addition to that, the canalicular length and the density of canaliculi of *Becn1* cKO mice showed significantly decreased (**Figure 2 & 3**). To evaluate whether *Becn1* regulates lacunae and canaliculi network in bone, the mRNA expression level of Perilacunar/ canalicular remodeling (PLR) enzymes including *MMP2*, *MMP13*, *MMP14*, *CtsK* and *MMP9*, were measured utilizing RT-qPCR. The relative mRNA expression of all of these genes in *Becn1* knockdown MLO-Y4 has substantially reduced as compared to the control cells (**Figure 4**). Addition to that, the protein *CtsK* expression in both *Becn1* knockdown in osteocyte cell and control cell were evaluated to quantify protein from Western blot (**Figure5**). Consistent with RT-qPCR data, the protein expression of *Ctsk* has substantially reduced. Therefore, our findings suggest that *Becn1* plays a critical role in perilacunar/ Canalicular remodeling in bone matrix.

3.2 Establishment of stably knockdown *Becn1* in MLO-Y4 cell line using lentiviral shRNA

After stably knock down *Becn1* in MLO-Y4 osteocyte-like murine cell line infecting using lentiviral shRNA, the cell morphologies and the cell proliferation has been observed (**Figure 6**). MLO-Y4 has star shaped and retain osteocyte morphology. Interestingly, once the *Becn1* knockdown in MLO-Y4 cell, it displayed similar to epithelial-like shape. Western Blot assay was performed to validate the protein expression level of *Becn-1* as shown in **Figure 7**. Furthermore, the mRNA expression level of *Becn-1* has markedly decreased validated by RT-qPCR more than 70 % of infected cells were detected after puromycin selection. (**Figure 8**). After confirming the knockdown of *Becn-1* gene in MLO-Y4 cell, the cells were used for further *in vitro* studies.

3.3 Expression of osteocyte-specific markers in *Becn-1* knockdown in osteocyte

To further investigate the effect of the *Beclin1* knockdown on osteocyte-related genes, we performed RT-qPCR to obtain mRNA expression level of osteogenic markers, including *Colla1*, *Col3a1*, *CtsK*, *MEPE*, *fgf23*, osteoclastic markers, *CtsK* and *MMP14*, and osteoblastic markers, *RANKL*, *OPG* and *DMP1* for this study. Interestingly, the mRNA expression level of *Beclin1* knockdown in MLO-Y4 has markedly decreased in osteoclastic gene, *CtsK*, *Mmp13* and *Colla1*, *Col3a1* and *fgf23* as compared to control cell, which shown in **Figure9**. Similar to that, all of the osteogenic gene expression has significantly decreased in *Beclin1* knockdown MLO-Y4 cells. Conversely, we observed that the expression level of osteoblastic markers, *RANKL*, *OPG*, and *DMP1* has significantly increased in *Beclin1* knockdown MLO-Y4.

3.4 Beclin1 knockdown in osteocyte cell line suppress autophagic pathways in bone homeostasis

As autophagic pathways in bone biology plays an important role in bone mineralization and bone resorption, we further investigated whether knock down of Beclin-1 in osteocyte-like cell line MLO-Y4 suppresses the autophagic pathway in bone physiology. First, we employed RT-qPCR to examine the mRNA expression level of important ATG-related genes. ATG markers that are widely used to visualize isolation membranes are *ULK1 (Atg1)*, *ATG5*, and microtubule-associated protein light chain 3 (*LC3/Atg8*) and the mRNA expression level of these genes were measured. The expression of all Atg-related genes is significantly reduced in Beclin1 knockdown MLO-Y4 when compared with control MLO-Y4 (**Figure 11 & 12**). Although expression of *Atg 101* has slightly increased in Beclin1 KD cell, the statistic was not significant. Next, we then utilized Western blot to detect LC3 protein, upon reduction of Beclin1 gene expression in osteocyte cell (**Figure 10**). Not only LC3 protein is extensively used to monitor the autophagy, but also it is an important marker to detect LC3 conversion (LC3-I to LC3-II) by immunoblotting analysis since the amount of LC3-II is clearly correlated with the number of phagosomes (Noboru *et al.*, 2007). Endogenous LC3-I is found in the cytoplasm, whereas LC3-II is conjugated with phosphatidylethanolamine (PE) that is present in isolation membranes and autophagosomes. Consistent with the previous data, the LC3 II protein expression has significantly decreased in Beclin1 knockdown in MLO-Y4, whereas LC3-I is not affected, as compared to the control cell. Herein, we can conclude that the degradation of LC3-II is completely inhibited whereas LC3-I is not affected. Based on our data, mRNA expression of most Atg-related proteins has been significantly decreased and potentially inhibits the upstream

autophagic pathway in the ECM upon reduction of Beclin1 gene expression in MLO-Y4.

Therefore, we can conclude that Beclin1 plays a critical role in induction of autophagic pathway in bone homeostasis.

3.5 TGF- β boosts cell-intrinsic Osteocytic PLR/ Canalicular remodeling

The transforming growth factor beta (TGF- β) pathway is one of the crucial signaling pathways that is responsible to regulate bone mass and quality, which is produced by bone-forming osteoblasts that sequestered in the ECM in an inactive form (Sinha *et al.*, 1998). A recent study conducted by Dole *et al.* demonstrated that the TGF- β acts directly on osteocytes to control their perilacunar/canalicular matrix and maintain the lacuna-canalicular network in bone matrix. To examine the cell-intrinsic effects of TGF- β on Beclin-1 knockdown MLO-Y4 osteocyte-like cells, which mimic osteocytic gene expression, we employed RT-qPCR to measure the gene expression of matrix metalloproteinases (Mmps; namely Mmp2, Mmp9, Mmp13, and Mmp14), cathepsin K (Ctsk) and Serpine 1. Within 72 hours of treatment, clearly TGF- β induced expression of Mmp2, Mmp9, Mmp13 and Mmp14 and Ctsk in MLO-Y4 (**Figure 13**). This indicates that the TGF-Beta induces PLR in an osteocyte-intrinsic manner. Then we further investigate whether Beclin1 is strongly associated with the osteocytic PLR mechanism. Under same circumstances, Beclin1 knockdown in MLO-Y4 also treated with TGF- β , our study revealed that TGF- β also induced expression of Mmp2, Mmp9, Mmp13, Mmp14 and serpine1, but not CtsK. Furthermore, the induction ratio of TGF-beta treatment in Becn1 KD and control cells were examined, which shown in **Figure 14**. Although, the induction ratios of TGF- β treatment are not significant, but we observed that the induction ratio of all PLR markers in Becn1 KD cells are slightly reduced in Mmp2, Mmp9, and Mmp13 except

Serpine. Based on this data, Serpine is TGF— β dependent protein. Whereas the induction ratios of Mmp14 and CtsK upon TGF— β treatment in MLO-Y4 Becn1 KD cells were reduced 2-fold, which indicates that Mmp14 and Ctsk are Beclin-1 mediated regulation.

4. Discussion

Several studies have identified that Atg-related proteins including Beclin1 are closely involved in osteoclast and osteoblast mechanism in bone homeostasis (Shapiro *et al.*, 2014). This study advances our understanding of bone homeostasis by exploring the role of Beclin1 in osteocytes in terms of autophagic pathway as well as TGF— β signaling pathway.

A study revealed that the Lacunar-canalicular network (LCN) interconnected network of cells are to be potentially relevant to mechanical sensing and essential for signaling and solute transport (Wang *et al.*, 2013). Our *in vitro* study exhibited that the mRNA of all of matrix-degrading enzymes, including Mmp2, Mmp9, Mmp13, Mmp14, and CtsK reduced significantly in Becn1 deficient osteocyte in contrast to pure MLO-Y4 cells. Consistent with the data, the Silver-nitrate-Stained images of Becn1 cKO revealed that both canalicular density and canalicular length was two-fold decreased. Superficially, the size of canaliculi has distinctively increased in Becn1 cKO and potently due to the deficiency of lacuna-canalicular networks. In relation to that, current studies found that branching of the canaliculi at various distances from the lacunae further increases the density of the LCN network in the mineralized matrix and the larger numbers of canaliculi make their porosity space some 2.5-fold higher than the lacunar porosity (Boltel *et al.*, 2021). The lacuna-canalicular system in allows for canalicular fluid flow and signaling factors such as TGF-beta to and from the osteocytes via circulation. Our finding is also supported by the other study that among DMP-1 conditional TGF— β receptor deletion, also

led to reducing the canalicular network length and reduced expression of matrix-degrading enzymes that are necessary for perilacunar/canalicular remodeling without affecting lacunar morphology (Dole *et al.*, 2017). For our future direction, it will be crucial to further quantify the proliferation rate and the apoptotic rate of osteocyte in the histological staining of two *in vivo* models, which will provide deeper insights into the osteocyte development and maintenance in bone remodeling. The proliferation rate of osteocyte in histological staining should be examined using Ki67 and BrdU markers for *in vivo* study and to quantify the cell proliferation *in vivo*, minimum of 3 femoral cortical bone sections of both *Becn1* cKO mice as well as the control mice should be collected. Then the % proliferation using Ki67 or BrdU marker will be calculated by the number of dividing osteocytes divided by total number of both dividing and non-dividing osteocyte cells in the section. Additionally, the terminal transferase-mediated nick end labeling technique (TUNEL) assay should be utilized to detect the apoptotic osteocyte rate for in the femoral cortical tissue sections of *Becn1* cKO mice. The apoptotic rate of osteocyte would be calculated from at least three femoral cortical tissue samples of two models, the apoptotic index should be calculated by dividing the number of apoptotic osteocytes by the total number of intact osteocytes in the sections.

When *Becn1* expression is suppressed in osteocytes *in vitro*, we noted changes in osteocyte phenotypes. MLO-Y4 cells displayed dendrite-like structures which consist of several projections and elongated morphology whereas *Becn-1* knockdown in MLO-Y4 exhibited more spindle-like shape and lost their projection morphology (**Fig.4**). Previous study showed that *Becn-1* functions as a tumor suppressor gene (Delaneyet *et al.*, 2020 and Quet *et al.*, 2003). Indeed, as the autophagic pathway is suppressed in some physiological processes in tumor cells, the cell proliferation rate increases; therefore, it potently exhibits similar cellular morphology in the *Becn1* deficient MLO-Y4 cells.

We further examined the role of *Becn1* in genes related to osteocytes. Our *in vitro* study utilizing RT-qPCR revealed that, distinctly the relative mRNA expression of *MEPE*, *Mmp13*, *CtsK*, *Col1a1*, *Col3a1*, and *fgf23* has significantly decreased upon reducing the expression of *Becn1* in MLO-Y4. Conversely, the expression level of *RANKL*, *OPG* and *DMP1*, which are osteoblastic markers in mammalian cell, has markedly increased in *Becn1* knockdown MLO-Y4 cells (**Fig. 7**). Therefore, our study highlights that the *Becn1* in osteocytes play significant role in bone homeostasis by regulating both osteoblast-related genes and the osteoclast-related genes in bone extracellular matrix.

As *Becn-1* is known to be a master regulator of autophagic pathway, we speculate that reducing the *Becn-1* expression in osteocyte-like cell line also play critical role to suppress the autophagic pathway. Consistent with our hypothesis, *in vitro* study displayed that the relative mRNA expression of Atg-related proteins has predominantly reduced in absence of *Becn1* expression in MLO-Y4 cells. Specifically, *ULK1 (Atg1)*, *Atg5*, and microtubule-associated protein light chain 3 (*LC3/Atg8*) are crucial Atg-related proteins to visualize isolation membrane and these proteins detach before the completion of the autophagosome except LC3 (Yoshii et al., 2017). For better understanding, these isolation membrane markers are resided on the outer membrane, whereas LC3 and associating p62/SQSTM1 are bound to both outer and inner membranes of the cell. Not surprisingly, our RT-qPCR data showed that expressions of these genes decline in *Becn1* knockdown MLO-Y4 cells. Since the relative expression of all other Atg-related proteins that associated in the autophagic pathway, this suggests that *Becn1* is a master regulator of Atg-related protein which plays pivotal role in upstream of Atg pathway in bone homeostasis. Additionally, we observed that the degradation of LC3-II is completely inhibited whereas LC3-I is not affected in the absence of *Becn1* in MLO-Y4 cells (**Fig.8**). Taken together,

our findings highlight that the *Becn1* is a key player in autophagic pathway in skeletal homeostasis.

Not only TGF— β pathway plays crucial signaling pathway to regulate the bone osteoclasts and osteoblasts, but osteocytes also participated in PLR (Bonewald, 2009). Dole *et al.*, demonstrated that osteocyte-specific inhibition of TGF— β signaling reduced the expression of PLR gene expression, proving that osteocyte-intrinsic TGF— β signaling maintains bone quality through perilacunar/canalicular remodeling. Consistently, our finding showed that upon TGF— β treatment, both control and *Becn1* KD cells proved significantly higher PLR gene expressions than the control cells. Furthermore, the induction ratios of TGF— β treatment displayed that all the PLR markers are TGF— β independent except *serpine1* (**Figure 14**). However, the induction ratios of *Mmp14* and *Ctsk* in MLO-Y4 *Becn1* KD cells were reduced even more than other PLR markers, approximately 2-fold, which indicates that *Mmp14* and *CtsK* are *Beclin1* mediated regulation. This finding suggests that the TGF— β induced expression of *Mmp2*, *Mmp9*, *Mmp13* and *Mmp14* in both MLO-Y4 cells and *Becn1* knockdown MLO-Y4 cells, but not *CtsK* in *Becn1* knockdown cells. In conclusion, this study suggests the *Becn1* is not associated in TGF— β signaling pathway in osteocyte. A recent study reported that fibroblast growth factor (FGF) signaling pathway in mature osteocyte also play a critical role in osteocyte survival and regulation of bone mass (McKenzie *et al.*, 2019). Therefore, our future study would require further investigation of the role of *Becn1* in FGF signaling pathway.

As a result of deletion of *Becn1* in autophagic mechanism, suppressed the expression of majority of Atg-related proteins as well as autophagy pathway. Both the length and the density of canaliculi in skeletal tissue positively correlated with secretion of PLR markers, *Mmp2*, *Mmp13*, *Mmp14*, *CtsK* and *Serpine 1* in lacunar-canalicular network. In conclusion, *Becn1* strongly

regulates the autophagy pathway and the lacuna-canalicular network, however, Becn1 might not involve in the TGF— β signaling pathway which is a fundamental for maintaining physiological bone homeostasis.

5. Figure Legends and Figures

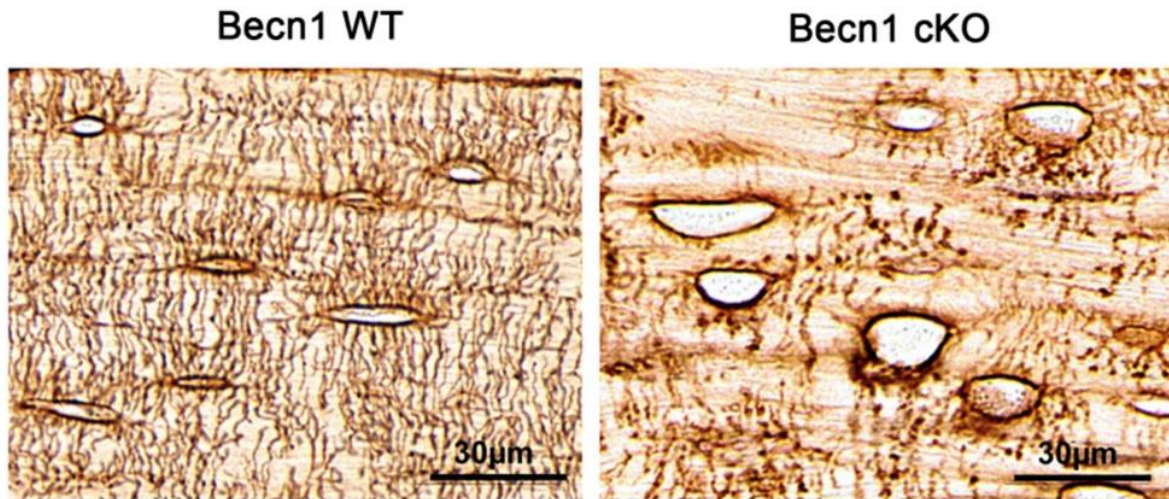


Figure 1. Silver-nitrate-Stained images of Becn1 WT (left) and Becn1 cKO (right).

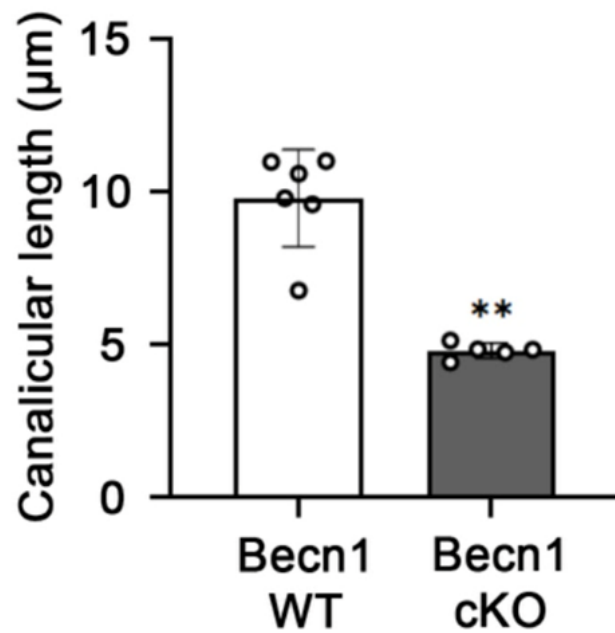


Figure 2. Canalicular length (μm) of Becn1 Wildtype and Becn1 conditional Knockout

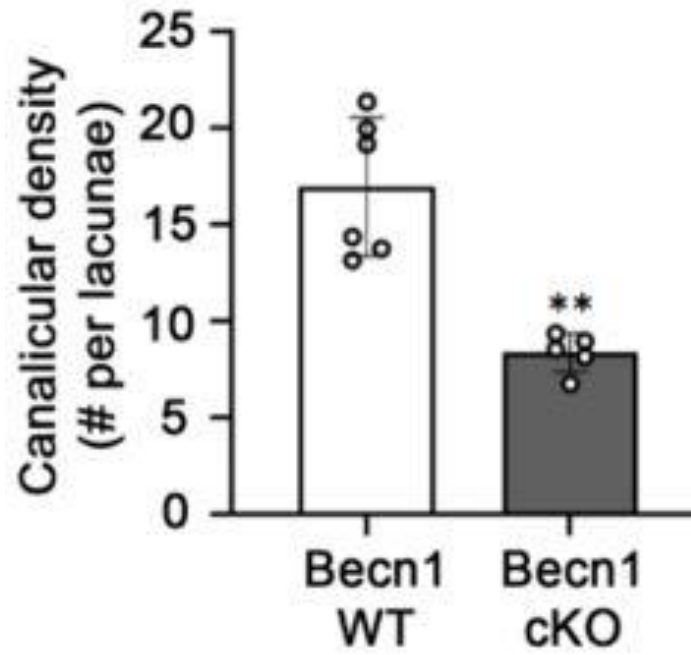


Figure 3. Quantification of canaliculus density (# per lacuna) of Becn1 Wildtype and Becn1 conditional Knockout

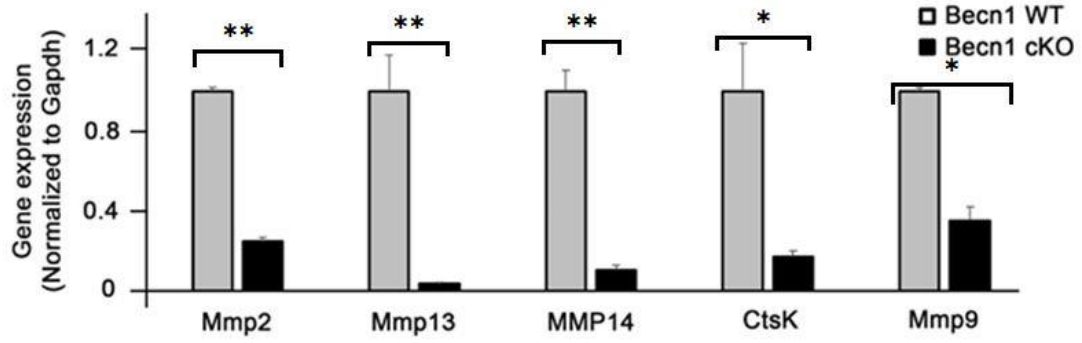


Figure 4. RT-qPCR analysis of the osteocyte genes MMP2, MMP13, MMP14, MMP9 and Ctsk in WT MLO-Y4 cells and Becn1 KD MLO-Y4 cells.

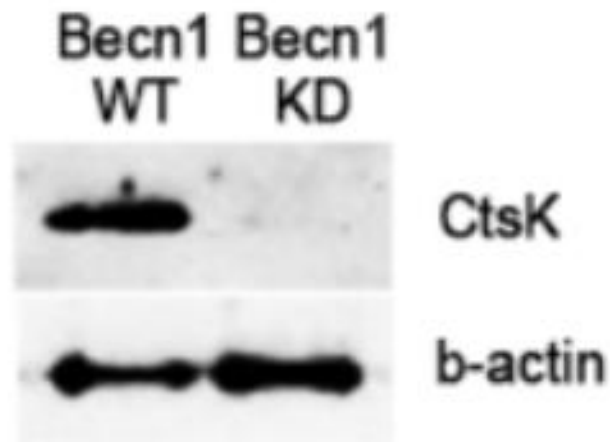


Figure 5. Western blotting of Ctsk in MLO-Y4 Becn1 KD cells and MLO-Y4.

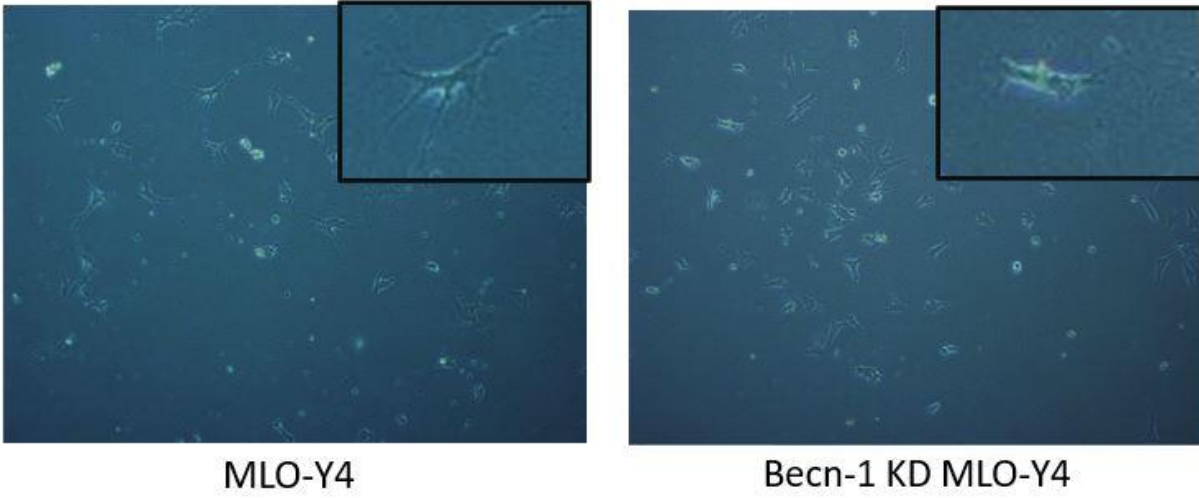


Figure 6. Cell morphology of MLO-Y4 and Becn-1 KD MLO-Y4 under the microscope.

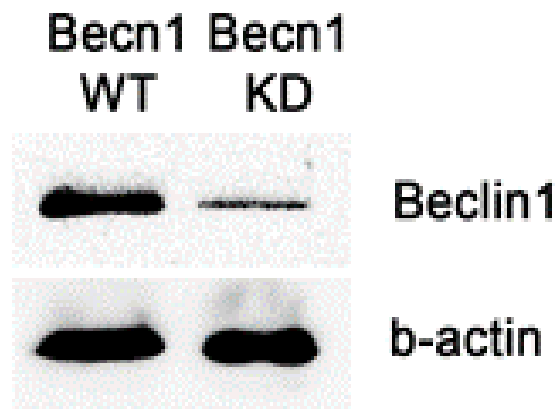


Figure 7. Western blotting of MLO-Y4 transfected with lentiviral shRNA Becn1 knockdown.

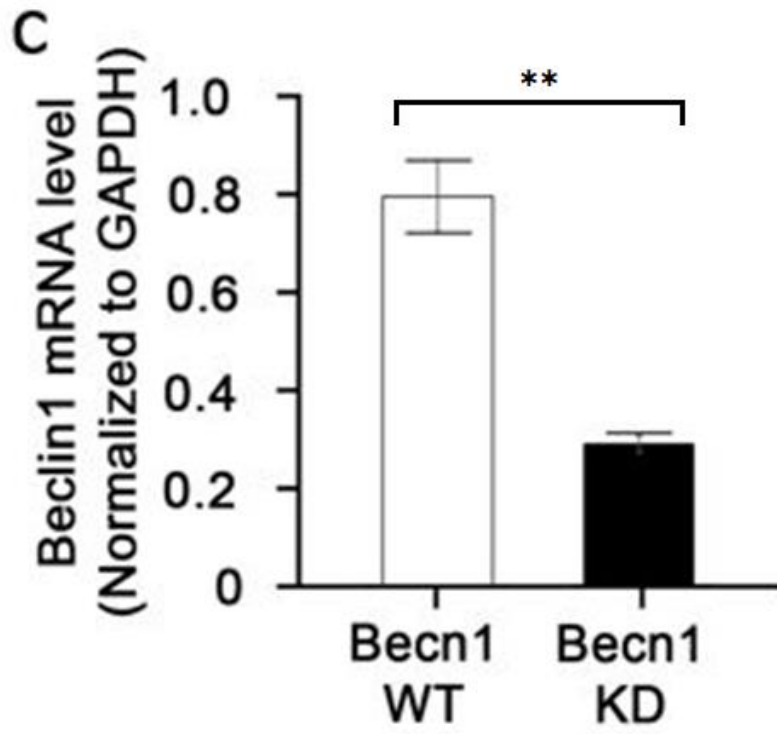


Figure 8. Gene expression of Beclin-1 mRNA by RT-qPCR following transfection with lentiviral shRNA Beclin

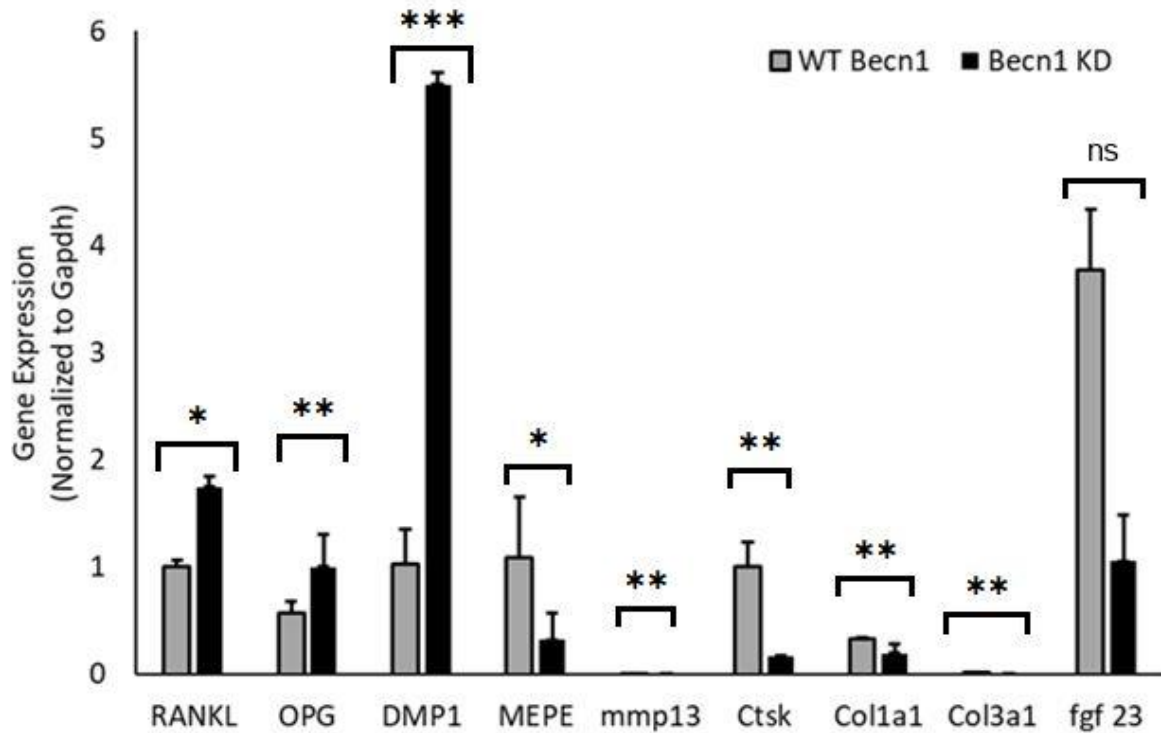


Figure 9. RT-qPCR analysis of the osteocyte genes (RANKL, OPG, DMP1, Mepe, mmp13, Ctsk, Col1a1, Col3a1 and fgf23) in WT MLO-Y4 cells and Becn1 KD MLO-Y4 cells.

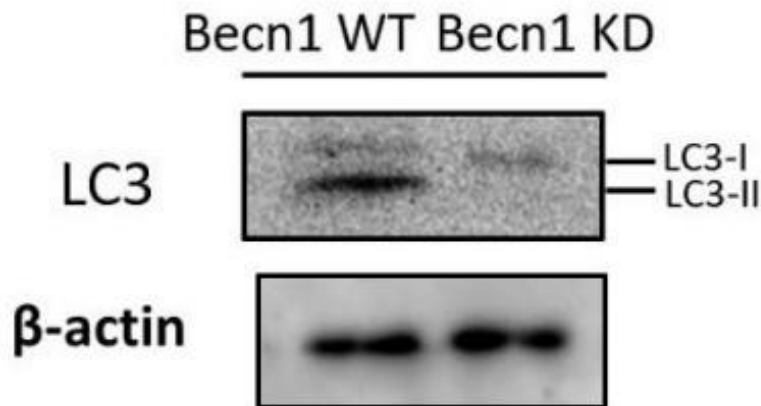


Figure 10. Western blotting of LC3 in MLO-Y4 Becn1 KD cell and MLO-Y4 cell.

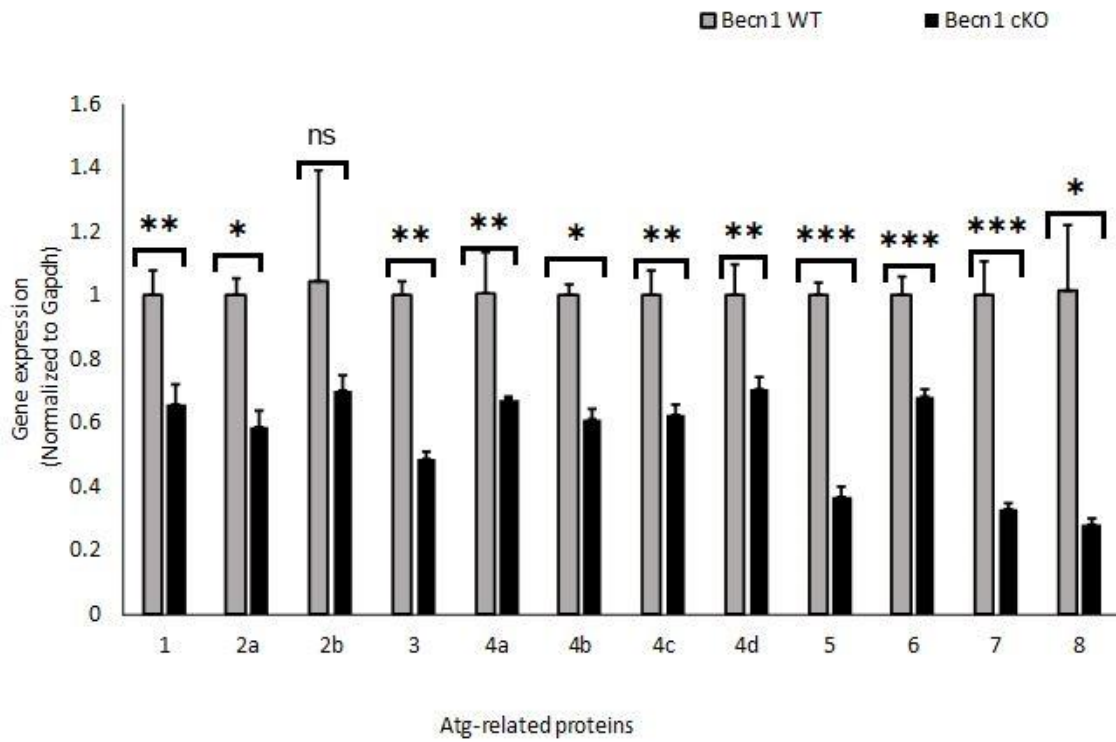


Figure 11. RT-qPCR analysis of the Atg-related genes (Atg 1 through Atg8) in WT MLO-Y4 cells and Bec1 KD MLO-Y4 cells.

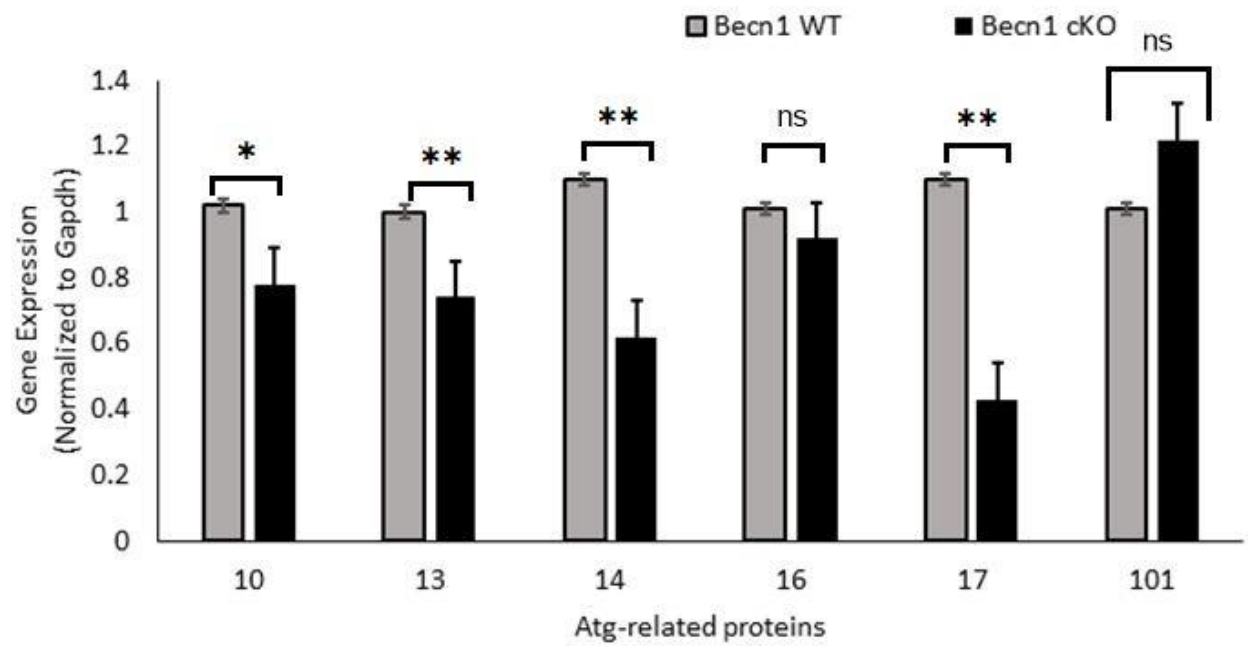


Figure 12. RT-qPCR analysis of the Atg-related genes (Atg 10 through 101) in WT MLO-Y4 cells and Becl1 KD MLO-Y4 cells.

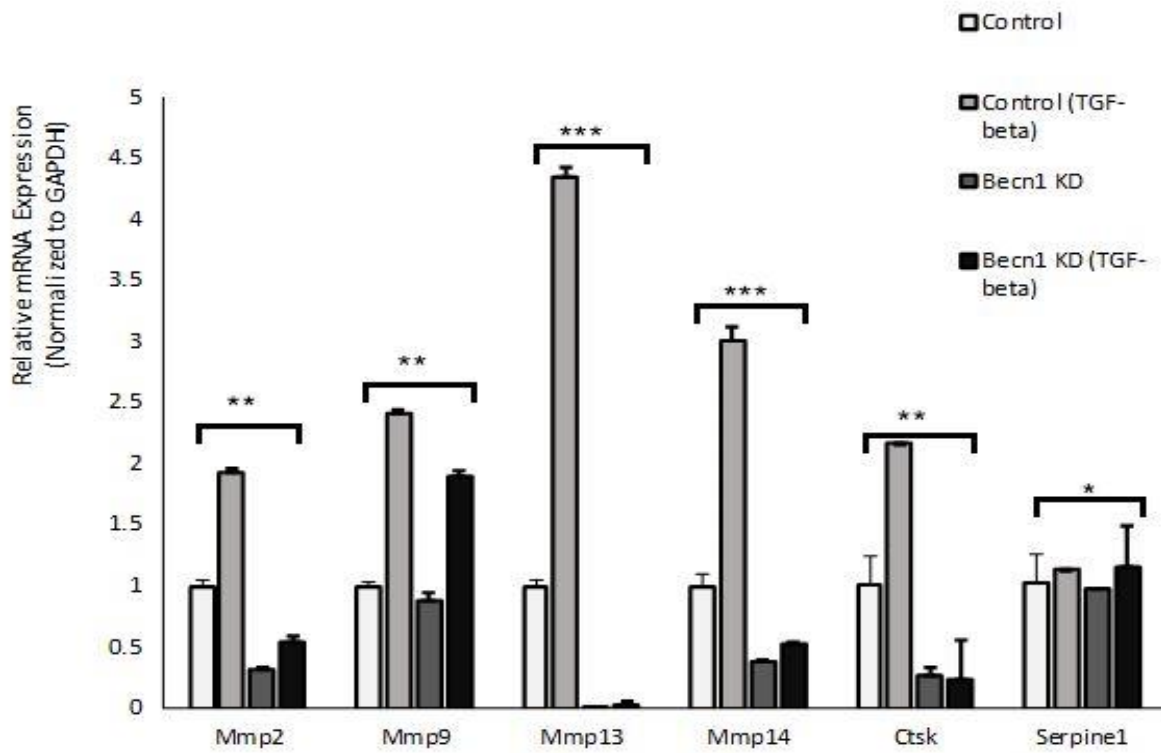


Figure 13. Effects of TGF-b in Becn1 KD MLO-Y4 cells and WT Becn1 MLO-Y4 cells.

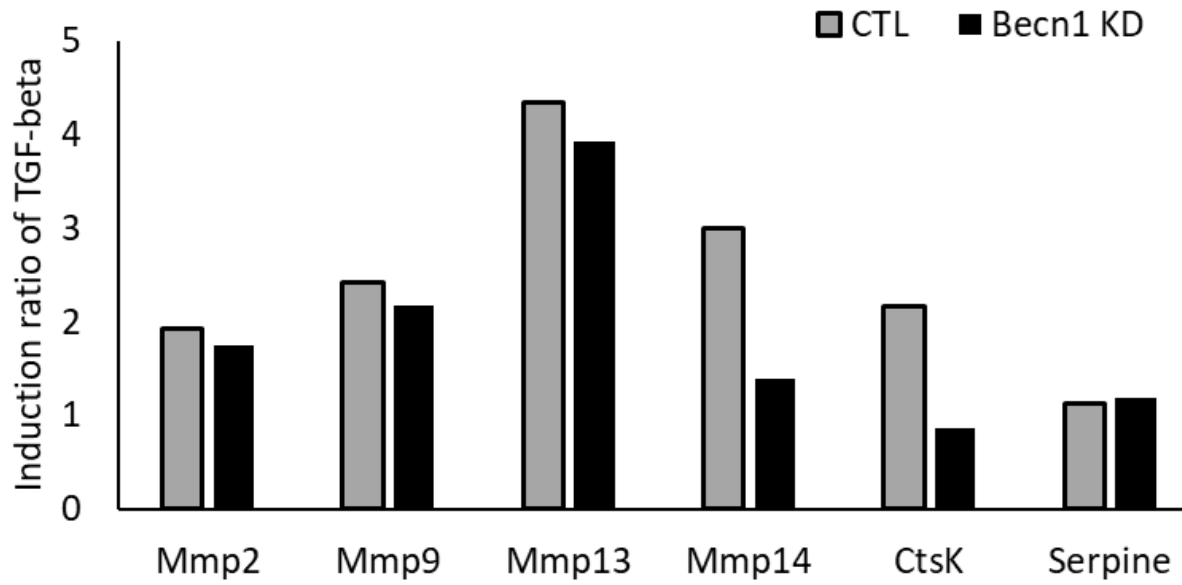


Figure 14. Induction ratio of TGF-beta treatment in Becn1 KD and Control cells.

Gene	Sequence (5'-3')	Amplicon (bp)
<i>GAPDH</i>	Forward: AGG TCG GTG TGA ACG GAT TTG Reverse: TGT AGA CCA TGT AGT TGA GGT CCA	62
<i>Atg6/Becn-1</i>	Forward: CAG GAA CTC ACA GCT CCA TTA C Reverse: CCA TCC TGG CGA GTT TCA ATA	77
<i>OPG</i>	Forward: CGA GTG TGT GAG TGT GAG GAA Reverse: TGT TTC GCT CTG GGG TTC	84
<i>RANKL</i>	Forward: TGA AGA CAC ACT ACC TGA CTC CTG Reverse: CCC ACA ATG TGT TGC AGT TC	84
<i>DMP1</i>	Forward: AAG CTG ACA GCG AGT CCA AC Reverse: GGG CCG ACT CCT GAC TCT	60
<i>Ctsk</i>	Forward: CTC CAT CGA CTA TCG AAA GAA AG Reverse: AAA GCC CAA CAG GAA CCA C	75
<i>MEPE</i>	Forward: GAT GCA GGC TGT GTC TGT TG Reverse: TGT CTT CAT TCG GCA TTG G	71
<i>MMP2</i>	Forward: TTG TTC TTT GAT GCA GTC AGC Reverse: GAT TTG CGC AAA AGT GC	65
<i>MMP9</i>	Forward: ACG ACA TAG ACG GCA TCC A Reverse: GCT GTG GTT CAG TTG TGG TG	72
<i>MMP13</i>	Forward: GCC AGA ACT TCC CAA CCA T Reverse: TCA GAG CCC AGA ATT TTC TCC	92
<i>MMP14</i>	Forward: GAG AAC TTC GTG TTG CCT GA Reverse: CTT TGT GGG TGA CCC TGA CT	78
<i>Col1a1</i>	Forward: ATG TTC AGC TTT GTG GAC CTC Reverse: GCA GCT GAC TTC AGG GAT GT	93
<i>Col3a1</i>	Forward: TCC CCT GGA ATC TGT GAA TC Reverse: TGA GTC GAA TTG GGG AGA AT	63

Table 1. Oligonucleotide osteocyte primer sets used for real-time RT-PCR.

Gene	Sequence (5'-3')	Amplicon (Bp)
Atg1/ Ulk1	Forward: GGA TCCATG GTG TCA CTG CA Reverse: CAA GGG CAG CTG ATT GTA CC	72
Atg2a	Forward: ATA TTC ACC TGG AAA CCT GGT C Reverse: CCT CGA TGG AGC TCA CAA A	93
Atg2b	Forward: TGC ACC CGG CAT CTT TAC Reverse: TGG ATT CAT CCA CTG AAG CA	63
Atg3	Forward: ATC ACC CCA GAA GAG TTT GTG Reverse: TCA ATT CTT CCC CTG TAG CC	85
Atg4a	Forward: GAA GGA AGT TTT CCC CGA TT Reverse: CCA CAG CGC AGC ATA CAT	73
Atg4b	Forward: CCT TGG CTG TTC ACA TAG CA Reverse: TGG CCC TGC ATA ACC TTC T	69
Atg4c	Forward: CTA TTT ATG TTG CCC AGG ACT GTA Reverse: AAA TAA TGA CAG CCT TGT CAC G	105
Atg4d	Forward: ACG TCT CTC AGG ACT GCA CA Reverse: CCA CTC CGC TGT AGG ATC TG	77
Atg5	Forward: AAG TCT GTC CTT CCG CAG TC Reverse: TGA AGA AAG TTA TCT GGG TAG CTC A	136
Atg6/ Beclin1	Forward: AGG ATG GTG TCT CTC GAA GAT T Reverse: GAT CAG AGT GAA GCT ATT AGC ACT TTC	77
Atg7	Forward: CCG GTG GCT TCC TAC TGT TA Reverse: AAG GCA GCG TTG ATG ACC	60
Atg8/LC3	Forward: CCC CAC CAA GAT CCC AGT Reverse: CGC TCA TGT TCA CGT GGT	104
Atg9a/Var1	Forward: TCC TTC TAC CTA CAT GCT CTT CG Reverse: TTC TGC GTC TGC ACA ATC C	92
Atg10	Forward: GCC AGT GTG CTC ACA TGT CT Reverse: TCG TCA CTT CAG AAT CAT CCA	70
Atg13	Forward: GAA GCA AGG GCA TGA ATA TGT Reverse: GCC TTC TCC TAA GCC ATT CAG	76
Atg16L1	Forward: GTC CGA GCT GTC AGC AGA Reverse: CGG ACA GAC CAA AGA TAT TAG TGA	91
Atg17/Rb1cc1	Forward: GGA AAT GCA AAA TGT CAG AAC C Reverse: TTT TCT TTC CTC ATT TTC TCT CTT G	90
Atg101	Forward: TTC ACC TAT GTG CGC GTC T Reverse: TGA GTT CCT CAG TGC ATC CTT	87

Table 2. Oligonucleotide autophagy primer sets used for real-time RT-PCR.

6. References

1. Asagiri M, Takayanagi H. The molecular understanding of osteoclast differentiation. *Bone*. 2007;40:251–64. Doi: 10.1016/j.bone.2006.09.023
2. Bortel, E., Grover, L.M., Eisenstein, N., Seim, C., Suhonen, H., Pacureanu, A., Westenberger, P., Raum, K., Langer, M., Peyrin, F., Addison, O. and Hesse, B. (2022), Interconnectivity Explains High Canalicular Network Robustness between Neighboring Osteocyte Lacunae in Human Bone. *Adv. NanoBiomed Res.*, 2: 2100090. <https://doi.org/10.1002/anbr.202100090>
3. Bonewald LF. Osteocytes as dynamic multifunctional cells. *Ann NY Acad Sci*. (2007) 1116:281-90. Doi: 10.1196/annals.1402.018
4. Bonewald LF. The amazing osteocyte. *J Bone Miner Res*. (2011) 26:229–38. doi: 10.1002/jbmr.320
5. Creecy, A., Damrath, J. G., & Wallace, J. M. (2021). Control of bone matrix properties by osteocytes. *Frontiers in Endocrinology*, 11. <https://doi.org/10.3389/fendo.2020.578477>
6. Dole, N. S., Mazur, C. M., Acevedo, C., Lopez, J. P., Monteiro, D. A., Fowler, T. W., Gludovatz, B., Walsh, F., Regan, J. N., Messina, S., Evans, D. S., Lang, T. F., Zhang, B., Ritchie, R. O., Mohammad, K. S., & Alliston, T. (2017). Osteocyte-Intrinsic TGF- β Signaling Regulates Bone Quality through Perilacunar/Canalicular Remodeling. *Cell reports*, 21(9), 2585–2596. <https://doi.org/10.1016/j.celrep.2017.10.115>
7. Fowler TW, Acevedo C, Mazur CM, Hall-Glenn F, Fields AJ, Bale HA, et al. Glucocorticoid suppression of osteocyte perilacunar remodeling is associated with subchondral bone degeneration in osteonecrosis. *Scientific Reports*. 2017;7:44618 Doi: 10.1038/srep44618.

8. J. R. Delaney et al., Autophagy gene haploinsufficiency drives chromosome instability, increases migration, and promotes early ovarian tumors. *PLoS Genet.* 16, e1008558(2020).
9. Lane NE, Yao W, Balooch M, Nalla RK, Balooch G, Habelitz S, et al. Glucocorticoid-Treated Mice Have Localized Changes in Trabecular Bone Material Properties and Osteocyte Lacunar Size That Are Not Observed in Placebo-Treated or Estrogen-Deficient Mice. *Journal of Bone and Mineral Research.* 2006;21:466–76.
10. McKenzie, J., Smith, C., Karuppaiah, K., Langberg, J., Silva, M. J., & Ornitz, D. M. (2019). Osteocyte Death and Bone Overgrowth in Mice Lacking Fibroblast Growth Factor Receptors 1 and 2 in Mature Osteoblasts and Osteocytes. *Journal of bone and mineral research : the official journal of the American Society for Bone and Mineral Research*, 34(9), 1660–1675. <https://doi.org/10.1002/jbmr.3742>
11. Noboru Mizushima & Tamotsu Yoshimori (2007) How to Interpret LC3 Immunoblotting, *Autophagy*, 3:6, 542-545, DOI: 10.4161/auto.4600
12. Sinha, S., Nevett, C., Shuttleworth, C.A. and Kielty, C. M. (1998). Cellular and extracellular biology of the latent transforming growth factor-beta binding proteins. *Matrix Biol.* 17, 529-545.
13. Fu L.-l., Cheng Y., Liu B. Beclin-1: Autophagic regulator and therapeutic target in cancer. *Int. J. Biochem. Cell Biol.* 2013;45:921–924. doi: 10.1016/j.biocel.2013.02.007.
14. Levine, B. & Kroemer, G. Biological functions of autophagy genes: a disease perspective. *Cell* 176, 11–42 (2019).
15. Maiuri MC, Le Toumelin G, Criollo A, et al. Functional and physical interaction between Bcl-X(L) and a BH3-like domain in Beclin-1. *EMBO J.* 2007;26(10):2527–39.

16. Kimmelman, A. C. & White, E. Autophagy and tumor metabolism. *Cell Metab.* 25, 1037–1043 (2017).
17. Pattingre S, Tassa A, Qu X, Garuti R, Liang XH, Mizushima N, Packer M, Schneider MD, Levine B. Bcl-2 antiapoptotic proteins inhibit Beclin 1-dependent autophagy. *Cell.* 2005 Sep 23;122(6):927-39. doi: 10.1016/j.cell.2005.07.002. PMID: 16179260.
18. Shapiro I.M., Layfield R., Lotz M., Settembre C., Whitehouse C. Boning up on autophagy: The role of autophagy in skeletal biology. *Autophagy.* 2014;10:7–19. doi: 10.4161/auto.26679.
19. Sharma D, Ciani C, Marin PA, Levy JD, Doty SB, Fritton SP. Alterations in the osteocyte lacunar–canalicular microenvironment due to estrogen deficiency. *Bone.* 2012;51:488–97. Doi: 10.1016/j.bone.2012.05.014.
20. Qing, H., and Bonewald, L.F. (2009). Osteocyte remodeling of the perilacunar and pericanalicular matrix. *Int J. Oral Sci.* 1, 59-65.
21. Qing H, Ardeshirpour L, Pajevic P, Dusevich V, Jähn K, Kato S, et al. Demonstration of osteocytic perilacunar/canalicular remodeling in mice during lactation. *Journal of Bone and Mineral Research.* 2012;27:1018–29. Doi: 10.1002/jbmr.1567.
22. X. Quet al., Promotion of tumorigenesis by heterozygous disruption of the beclin 1 autophagy gene. *J. Clin. Invest.* 112, 1809–1820 (2003)
23. Wang B, Zhou X, Price C, Li W, Pan J, Wang L. Quantifying load-induced solute transport and solute-matrix interaction within the osteocyte lacunar-canalicular system. *J Bone Mineral Res* (2013) 28:1075–86. doi: 10.1002/jbmr.1804
24. Wu, C., Zhang, S., Lin, L., Gao, S., Fu, K., Liu, X. ... Zhou, P. (2018). BECN1-knockout impairs tumor growth, migration and invasion by suppressing the cell cycle and partially

suppressing the epithelial-mesenchymal transition of human triple-negative breast cancer cells. *International Journal of Oncology*, 53, 1301-1312.

<https://doi.org/10.3892/ijo.2018.4472>

25. Yoshii, S. R., & Mizushima, N. (2017). Monitoring and Measuring Autophagy. *International journal of molecular sciences*, 18(9), 1865.

<https://doi.org/10.3390/ijms18091865>